International Journal of Research
Available at https://edupediapublications.org/journals
e-ISSN: 2348-6848
p-ISSN: 2348-795X
Volume 05 Issue 12
April 2018

Hybrid Fuzzy Controlled Isolated Micro Grid Based On Battery Storage System Using Renewable Energy Sources

Sana Shaik & M Divya Charitha

M-tech Student Scholar Department of Electrical & Electronics Engineering, CMR College of Engineering & Technology, Kandlakoya; Medchal Road, Hyderabad; Telangana, India.
Email: sanashaik02@gmail.com
Assistant Professor Department of Electrical & Electronics Engineering, CMR College of Engineering & Technology, Kandlakoya; Medchal, Hyderabad; Telangana, India.
Email: divyacharitha@gmail.com

Abstract- *The enabling of ac micro grids in distribution networks allows delivering distributed power and providing grid support services during regular operation of the grid, as well as powering isolated islands in case of faults and contingencies, thus increasing the performance and reliability of the electrical system. This paper proposes an alternative strategy to control the generated power within an isolated ac micro grid with distributed RES. The proposal is to control the terminal voltage of the existing battery banks below or equal its maximum allowable value. In this particular study, the power system consists of a power electronic converter supplied by a battery bank, which is used to form the ac grid (grid former converter), an energy source based on a wind turbine with its respective power electronic converter (grid supplier converter), and the power consumers (loads). The main objective of this proposed strategy is to control the state of charge of the battery bank limiting the voltage on its terminals by controlling the power generated by the energy sources. This is done without using dump loads or any physical communication among the power electronic converters or the individual energy source controllers. The electrical frequency of the micro grid is used to inform the power sources and their respective converters about the amount of power that they need to generate in order to maintain the battery-bank charging voltage below or equal its maximum allowable limit.. The Proposed concept is implemented to hybrid fuzzy controlled logic using mat lab/simulation link software.*

Index Terms—Battery banks, isolated micro grids, parallel inverters, power control, renewable energy sources (RESs), state of charge (SOC).

I. INTRODUCTION

Micro grids are becoming popular in distribution systems because they can improve the power quality and reliability of power supplies and reduce the environmental impact. Micro grid operation can be classified into two modes: grid-connected and islanded modes. In general, micro grids are comprised of distributed energy resources (DERs) including renewable energy sources, distributed energy storage systems (ESSs), and local loads [1–3]. However, the use of renewable energy sources such as wind and solar power in micro grids causes power flow variations owing to uncertainties in their power outputs. These variations should be reduced to meet power-quality requirements [4,5]. This study focuses on handling the problems that are introduced by wind power. To compensate for fluctuations in wind power, various ESSs have been implemented in micro grids. Short-term ESSs such as superconducting magnetic energy storage (SMES) systems [6], electrical double-layer capacitors (EDLCs) [7], and flywheel energy storage systems (FESSs) as well as long-term ESSs such as battery energy storage systems (BESSs) [8-9] are applied to micro grid control. ESSs can also be used to control the power flow at point of common coupling in the grid-connected mode as well as to regulate the frequency and voltage of a micro grid in the islanded mode. Among these ESSs, BESSs have been implemented widely owing to their versatility, high energy density, and efficiency. Moreover, their cost has decreased whereas their performance and lifetime has increased.

In practice, BESSs with high performance such as smooth and fast dynamic response during charging and discharging are required for micro grid control. This performance depends on the control performance of the power electronic converter. Proportional-integral (PI) control is a practical and popular control technique for BESS control systems. However, PI control might show unsatisfactory results for nonlinear and discontinuous systems [10].

When properly applied, these new, distributed generation units (DG) offer significant benefit to the grid and to end users. However, merging DGs into the traditional grid is not without technological challenges. The traditional electrical grid was not designed for power generation sources distributed near the ends of the T&D grid. The successful integration of DG power sources requires the single-direction grid architecture of the past transition to a smarter and more agile bi-directional grid [11]. As DGs continue to gain traction in the electrical market, new thinking and new strategies around power generation, distribution and consumption will continue to emerge. One of the increasingly common tactics for merging DGs into the larger electrical grid is a new twist on an old electrical architecture known as the micro grid. Micro

International Journal of Research
Available at https://edupediapublications.org/journals
e-ISSN: 2348-6848
p-ISSN: 2348-795X
Volume 05 Issue 12
April 2018

grids are areas of the grid that can operate as part of the larger macro grid or operate autonomously as a standalone system. The micro grid systems help facilitate the integration of DG assets into the larger electrical grid. Further, when properly implemented, micro grids can unlock a wide array of stacked values for grid operators and electrical consumers [12-13].

II. SYSTEM DESCRIPTION

Fig. 1 illustrates the simplified diagram of a stand-alone micro grid used to explain the control strategy proposed in this paper. It consists of a GFC, a GSC, and a battery bank. The renewable energy source, in this particular study, is a variable speed wind turbine coupled to a permanent-magnet synchronous generator (PMSG). Depending on the system size, other energy sources and other storage energy systems can be distributed along the micro grid. The simplicity of this system is useful to show the feasibility of the proposed control strategy without losing generality.

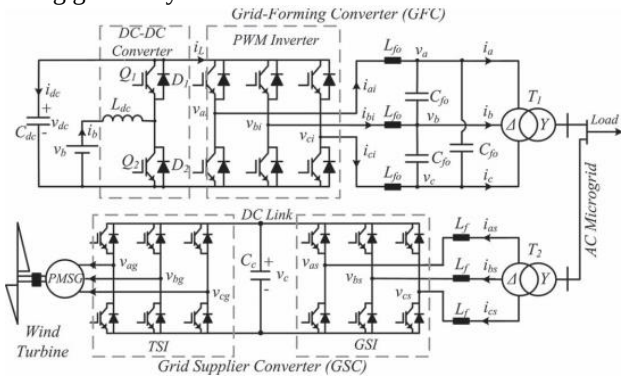

Fig. 1. Simplified diagram of the studied micro grid.

The GFC is a bidirectional converter formed by a pulse width modulation (PWM) three-phase inverter and a dc–dc converter that works in a buck mode when the battery bank is undercharge or in a boost mode when it is under discharge. The PWM inverter controls the magnitude and frequency of the micro grid

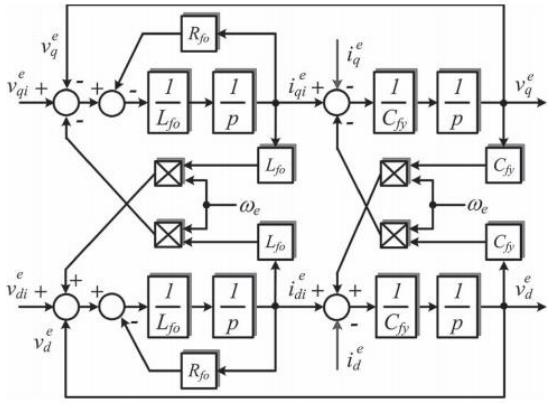

Fig. 2. Block diagram of LC filter implemented in a synchronous reference frame.

Voltage, while the dc–dc buck or boost converter is used to control the voltage at the dc bus capacitor (Cdc) which is the dc bus voltage as well as the charging and discharging of the battery bank.

The GSC is used to control the power generated by the renewable energy source. In this particular example, the converter is formed by a conventional back-to-back topology [12]. It has a grid-side PWM inverter (GSI) and a wind turbine-side PWM inverter (TSI). The GSI is used to control the dc-link voltage of the back-to-back topology, and the TSI is used to control the power generated by the wind turbine based on a maximum power point tracker (MPPT) algorithm.

III. GRID FORMER CONVERTER

A. Control of the Micro grid Voltage and Frequency

The micro grid voltage controller uses the traditional configuration implemented on a synchronous dq reference frame, with an inner current loop and an outer voltage loop [7]. The frequency and voltage reference values are calculated using droop control strategy as a function of the active and reactive powers, respectively, at the grid former converter terminals. The dq model of the LC filter in the delta side of transformer T1(see Fig. 1) is used to design the control loops of the GFC. The block diagram of this model is shown in Fig. 3, where Rfo is the equivalent series resistance of the filter inductor Lfo; be is the micro grid frequency in radians per second, the superscript's" denotes variables in the dq synchronous reference frame,ied and ie q are the dq currents in the delta side of transformerT1; Cfy is the per-phase equivalent capacitance of the LC filter and is equal to 3Cfo; and vqe and vde are the dq voltages in the capacitors of the LC filter. The subscript i denotes the output variables of the GFC PWM inverter. All the block diagrams shown in this paper use the operator p = d/dt. Based on the model presented in Fig. 2, an inner current loop and an outer voltage loop were designed, as illustrated in Fig. 3.

In this figure, "Λ" denotes estimated parameters, and GDID1 is the transfer function used to decouple at the sample instants the effect of the disturbances due to the load currents ieqe ied and the cross-coupling due to vq e and vd e. ZOH means zero-order hold (latch). Fundamentally, the current on the inductance Lf0

International Journal of Research
Available at https://edupediapublications.org/journals
e-ISSN: 2348-6848
p-ISSN: 2348-795X
Volume 05 Issue 12
April 2018

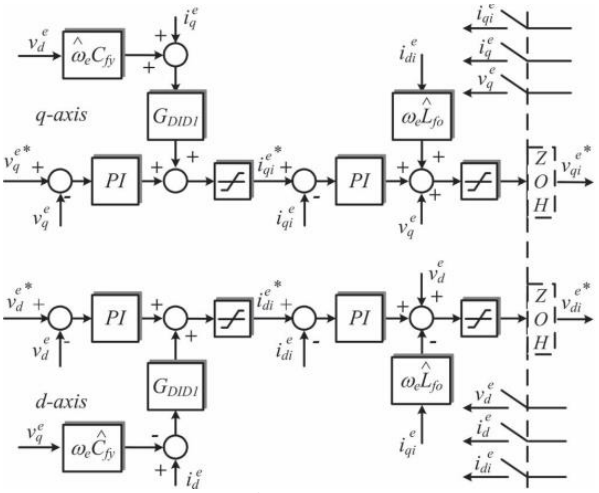

Fig. 3. Block diagram of the micro grid voltage controller.

is controlled in order to regulate the voltage on the capacitanceCf0, independently whether the power flux is from the PWMinverter to the micro grid or vice versa. The voltage reference values for the voltage controllers can be constant, generally equal to the nominal value of the micro grid voltage, or can be calculated based on a droop control strategy. In this paper, the voltage reference was fixed in 220 V(rms line voltage in the delta side of T1).

B. Control of the Bidirectional DC–DC Converter

The dc–dc converter (in GFC) is used to control the voltage in the capacitor Cdc. The action of the controller of thedc–dc converter can be considered equivalent to connecting a controlled voltage source, with mean value Vct, between the xy terminals of the converter circuit, as shown in Fig. 4(a) and (b).If the losses in the converter are not considered, the voltage on Cdc depends only on the difference between the power at the battery bank terminals (Pb) and (Pinv) which is the power at the terminals of the delta side of the isolation transformer T1,which is positive when the power flux is from the inverter to the grid and negative on the contrary. This is shown in Fig. 4(c).Therefore, the dynamic equation for vdc can be written as in(1), where wdc is an auxiliary variable defined by wdc = v^2dc

$$\frac{1}{2}C_{\mathrm{dc}}\frac{dv_{\mathrm{dc}}^2}{dt} = \frac{1}{2}C_{\mathrm{dc}}\frac{dw_{\mathrm{dc}}}{dt} = P_b - P_{\mathrm{inv}} \quad (1)$$

From (1) and Fig. 4, the dc bus voltage controller of the GFC can be designed with an inner current loop to control the battery bank current (ib) and an outer voltage loop to control the voltage over the capacitor Cdc, as illustrated in Fig. 6.

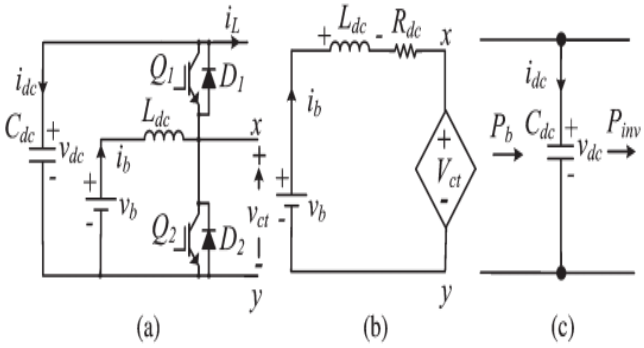

Fig. 4. DC–DC converter average model: (a) Original circuit, (b) equivalent average circuit of inductor and battery bank, and (c) average model of the bus dc.

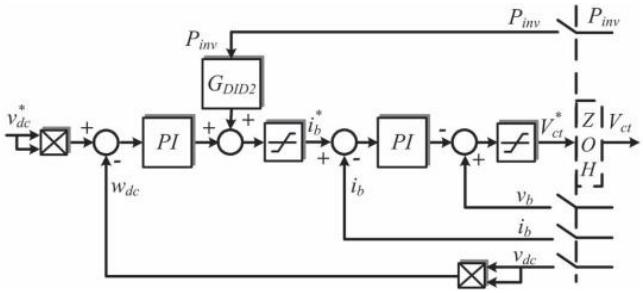

Fig. 5. Block diagram of the voltage controller of the dc–dc converter.

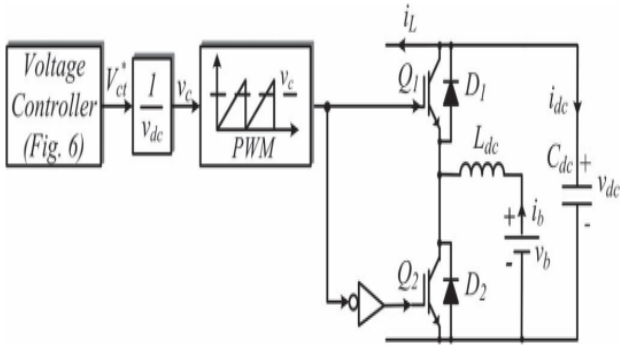

Fig. 6. Block diagram of the commands for the switches of the dc–dc converter.

GDID2 is used to decouple the power disturbance from the output of the inverter over the dc bus voltage. The output of the voltage controller (Vct) is the reference value for the PWM block used to generate the control signal forQ1 or Q2 switches, as shown in Fig. 6 [4].In Fig. 6, when Pinv is positive, the battery bank supplies the load, and the dc–dc converter functions on the boost mode using the Q2 switch and D1 diode. On the other hand, when Pinv is negative, the dc–dc converter functions on the buck mode using the Q1 switch and D2 diode.

IV. GRID SUPPLIER CONVERTER

A. Control of the Injected Current in the Microgrid and the Voltage at the DC Bus

In this paper, the GSI of the GSC (see Fig. 1) is used to control the dc bus voltage of the back-to-back topology.

International Journal of Research
Available at https://edupediapublications.org/journals
e-ISSN: 2348-6848
p-ISSN: 2348-795X
Volume 05 Issue 12
April 2018

This controller uses an inner current loop to control the injected current in the micro grid. The current controller is implemented in a dq synchronous reference frame aligned with the micro grid positive sequence voltage vector. The converter variable synchronization is done by using a synchronous phase-locked loop (PLL) that has a second-order resonant filter tuned for the fundamental frequency of the micro grid.

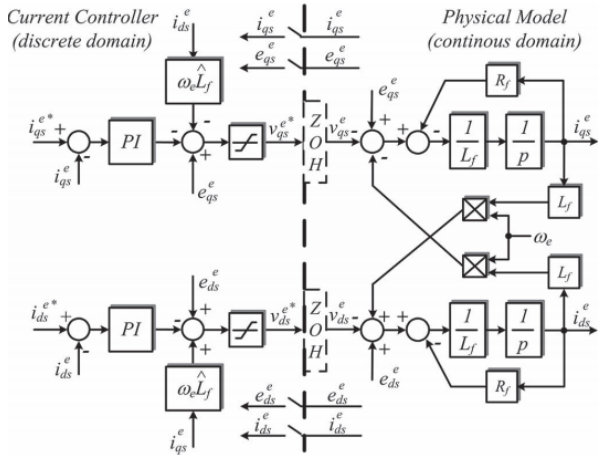

Fig. 7. Block diagram of the control of the injected current in the micro grid by the GSC.

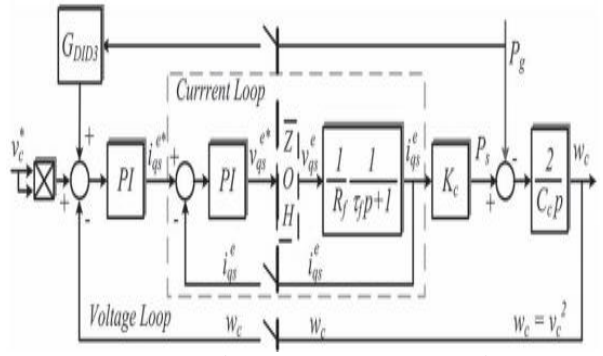

Fig. 8. Block diagram of the dc bus voltage controller for the GSC.

This PLL also has a module to extract the instantaneous positive and negative symmetrical components of the voltage of the micro grid [13]. The PLL was tuned based on its small signal analysis model for a bandwidth of 100 Hz. The block diagram of the current controller together with the filter (Lf) model in a synchronous reference frame is illustrated in Fig. 8, where Rf is the equivalent series resistance of the inductor Lf, ie qs and ie ds are the currents in the delta side of transformer T2, and eeqs and eeds are the dq axis components of the micro grid voltage. The adopted current direction references are the same as those shown in Fig. 1.If the losses in the GSI and in the inductor Lf are neglected, the variation of the energy stored in the capacitor Cc is equal to the difference between the active power received from themicrogrid (Ps) and the active power generated by the wind turbine (Pg). Using the convention of Fig. 2, this can be expressed as in

$$\frac{1}{2}C_c\frac{dw_c}{dt} = P_s - P_g; w_c = v_c^2 \quad (2)$$

For a dq synchronous reference frame aligned with themicrogrid voltage vector, it follows that ee ds = 0. Therefore, sis equal to (3/2) Esie qs, with Es being the magnitude of the phase voltage, considered constant in this application. By defining Kc equal to (3/2Es), the dynamic equation for the capacitor Cc is presented in

$$\frac{dw_c}{dt} = \frac{2}{C_c}\left(K_c i_{qs}^e - P_g\right) \quad (3)$$

The block diagram for the dc bus voltage controller is illustrated in Fig. 8. GDID3 is the transfer function used to decouple at the sample instants the effect of the disturbances due to Pg, and τf is the time constant Lf /Rf. The output of the voltage controller is the reference current (ie qs ∗) for the inner current loop.

V. PROPOSED STRATEGY TO CONTROL THEGENERATED POWER IN THE MICROGRID

In stand-alone and distributed renewable energy systems, there is no commercial or conventional grid to absorb any surplus power generated internally in the micro grid. Therefore, the generated power needs to be controlled when the load power is less than the amount of power that could be generated by the energy sources. This is necessary to keep the energy balance in the micro grid under control and to keep the battery bank voltage below or equal its maximum allowable value. This is necessary since voltages higher than the gasification voltage can decrease the life span of batteries or even damage them irreversibly [17].In the proposed control strategy, the GFC verifies the battery bank voltage to know if it reached the maximum allowed charging voltage and, if so, change the micro grid frequency to inform the other sources that they must reduce their generated power. Based on the micro grid frequency, the control systems of the power generation sources connected to the micro grid decide whether to restrict the power generated by each of them.

This control strategy can be explained based on Fig.9. While the terminal voltage of the battery bank is below its maximum limit, the micro grid frequency (f) is determined according to the conventional droop control strategy, described by line C1 inFig.9, since a physical or virtual inductance is added when the line resistance cannot be neglected [7]. The frequency value is calculated by (8), where kp is the slope constant of the line C1.On this situation, there are no restrictions about the amount of

International Journal of Research
Available at https://edupediapublications.org/journals
e-ISSN: 2348-6848
p-ISSN: 2348-795X
Volume 05 Issue 12
April 2018

power that can be generated, and the existing renewable energy sources can function on their maximum power point. Obviously, this is true only if the battery bank has been designed with sufficient capacity to absorb all the power that the renewable sources can produce at a given instant

$$f = f_0 - k_p P_{\text{inv}}$$

On the other hand, if the maximum voltage of the battery bank is reached, the micro grid frequency is imposed to be always higher than the value fmax, which is the maximum frequency of operation of the conventional droop control strategy. This is illustrated by the hatched area in Fig.9. Now, the value of the frequency (f) is a variable that changes dynamically

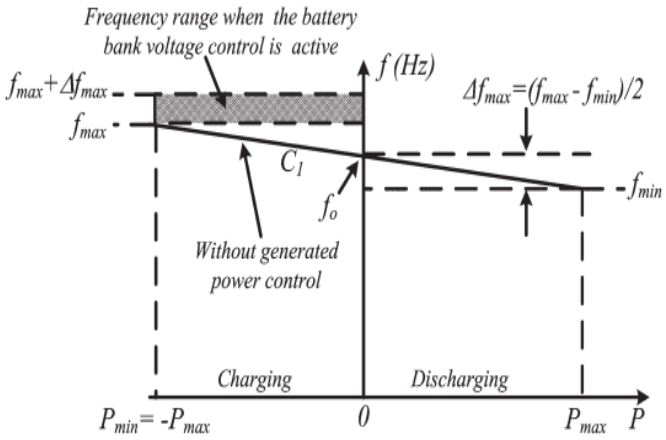

Fig. 9. Frequency versus power in the GFC based on the proposed power control.

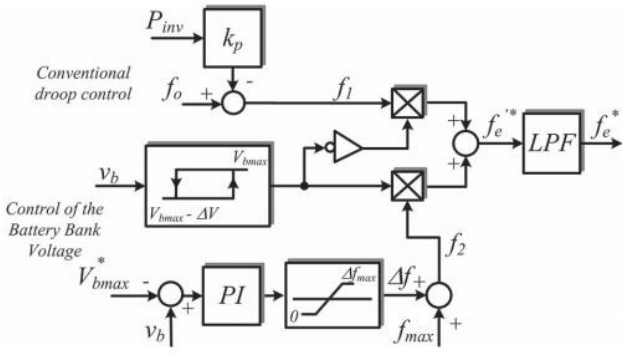

Fig. 10. Block diagram of the frequency control at the GFC.

With the terminal voltage of the battery bank (vb), the power generated internally in the micro grid (Pg), and the power of the GFC (Pinv). This can be expressed by (9). As the calculation of the frequency depends on the dynamics of the battery bank voltage controller, its relationship with the power (Pinv) does not follow a well-defined algebraic equation as, for example, a straight line. Therefore, Fig. 3 shows only an illustration that the frequency can assume any value between fmax and fmax +Δfmax. In this operating condition, it is necessary to restrict the amount of power that can be generated by renewable sources; otherwise, the integrity of the battery bank is at risk. The amount of power that needs to be reduced from the maximum power that each source is able to produce at every moment has a direct relation to the frequency difference Δf = f − fmax. The values of fo and ±Δfmax adopted in this work are 60 Hz and ± 0.60 Hz so that the frequency range of the micro grid is between 59.4 Hz (fmin) and 61.2 Hz (fmax + Δfmax).

$$f = f_{\max} + \Delta f(v_b, P_g, P_{\text{inv}})$$

A. Implementation of the Proposed Strategy in the GFC

The control of the battery bank voltage, in order to ensure its integrity, was implemented as shown in Fig. 10. While the output of the hysteresis loop is zero, the value of the frequency reference is fe ∗ = f1. On the other hand, while the output of the hysteresis loop is one, a proportional and integral (PI) controllers used to regulate the terminal voltage of the battery bank equal or below its maximum allowed value (Vbmax). The output of

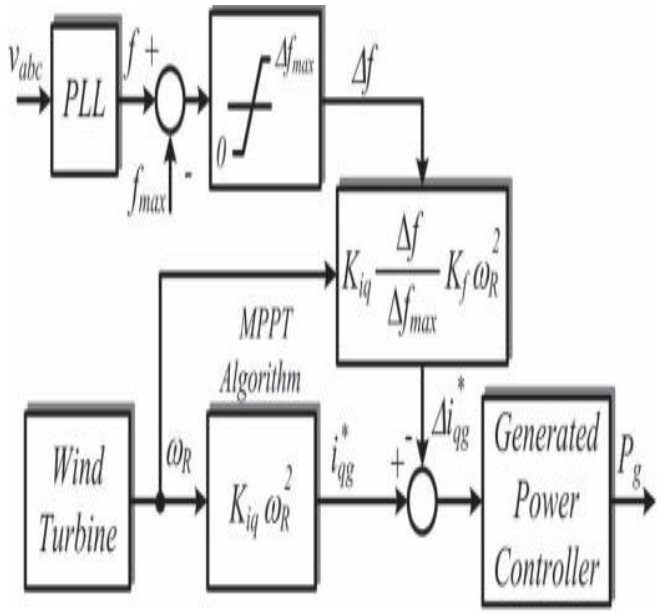

Fig. 11. Block diagram of the power control at the GSC.

International Journal of Research
Available at https://edupediapublications.org/journals
e-ISSN: 2348-6848
p-ISSN: 2348-795X
Volume 05 Issue 12
April 2018

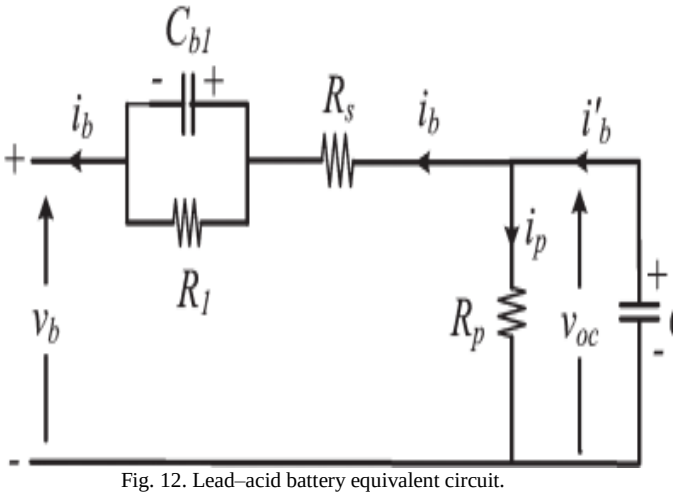

Fig. 12. Lead–acid battery equivalent circuit.

This controller is the increment of frequency (Δf) that must be added to the value fmax to form the new micro grid frequency reference value (fe ∗ = f2 = fmax + Δf). The value of Δf is proportional to the amount of power that must be decremented from the generated power in order to control the battery bank terminal voltage. The low-pass filter with a 1-Hz bandwidth shown in Fig. 9 is used to avoid sudden variations in frequency due the hysteresis loop.

B. Implementation of the Proposed Strategy in the GSC

The grid frequency is measured by the GSC and if its value is higher than fmax, it means that the voltage of the battery bank is higher than its maximum allowed value. For the particular case where the renewable energy source is a wind turbine, the GSC power controller decrements the current reference i∗ q, originally calculated by (7), which is now calculated by (10), where Kfis a constant which serves to match the rated power of the GFC with the rated power of the wind turbine. The block diagram of this control action is presented in Fig. 11.

$$i_q^* = K_{iq}\left(1 - \frac{\Delta f}{\Delta f_{\max}} K_f\right)\omega_R^2$$

As the reference current is now determined by (10), the operating points of the wind turbine-generator set follow the dashed curve indicated by Tg in Fig. 8. This implies a reduction in the generator torque, which causes a reduction in power that is produced by the wind turbine keeping regulated the terminal voltage of the battery bank.

C. Tuning of the Battery Bank Terminal Voltage Controller

The tuning of the PI controller shown in Fig. 10 takes into account the dynamic of the battery bank. One possible model for lead–acid batteries is shown in Fig. 12. In this figure, voc is the battery open circuit voltage, Rs is the equivalent series internal resistance, R1 and Cb1 are used to model the over- or under voltage that happens when the battery is charging or discharging, Rp is the resistance due the natural losses, and Cbo models the battery capacity to storage energy. Normally, the natural losses occur very slowly, so the effect of Rp can be disregarded for the purpose of this work.

VI Hybrid fuzzy Logic controller

Fuzzy controllers demonstrate excellent performance in numerous applications such as industrial processes and flexible arm control.Mamdami's work introduced this control technology that Zadeh pioneered with his work in fuzzy sets. Unlike "two valued" logic, fuzzy set theory allows the degree of truth for a variable to exist somewhere in the range [0,1]. For example, if pressure is a linguistic variable that describes an input, then the terms low, medium, high and dangerous describe the fuzzy set for the pressure variable. If the universe of discourse for pressure is [0, 100], then low could be defined as "close to 10", "medium" is "around 40", and so on. For control applications, linguistic variables describe the control inputs for dynamic plants and rules define the relationships between the inputs. Thus, precise knowledge of a plant's transfer function is not necessary for design and implementation of the controller. The thrust of earlier efforts involved replacing humans in the control loop by describing the operators' actions in terms of linguistic rules.

There are two steps involved in the implementation of a fuzzy logic controller; fuzzification of inputs and determination of a "crisp output." Fuzzification involves dividing each input variable's universe of discourse into ranges called fuzzy subsets. A function applied across each range determines the membership of the variable's current value to the fuzzy subset. Linguistic rules express the relationship between input variables. Table I is an example of a matrix of rules to cover all possible combinations of fuzzy subsets for two input variables. In this case, each variable has seven subsets that gives a total of 49 rules. Defuzzification to determine the "crisp output", resolves the applicable rules into a single output value.

Table 1: PD Control Rule Matrix

Change In Error	Error						
	NB	NM	NS	ZO	PS	PM	PB
PB	ZO	PS	PM	PB	PB	PB	PB
PM	NS	ZO	PS	PM	PB	PB	PB
PS	NM	NS	ZO	PS	PM	PB	PB
ZO	NB	NM	NS	ZO	PS	PB	PB
NS	NB	NB	NM	NS	ZO	PS	PM
NM	NB	NB	NB	NM	NS	ZO	PS
NB	NB	NB	NB	NB	NM	NS	ZO

PID controllers are designed for linear systems and they provide a preferable cost/benefit ratio. However, the presences of nonlinear effects limit their performances. Fuzzy controllers are successful applied to non-linear system because of their knowledge based nonlinear structural characteristics. A FLC makes control decisions by its well-known fuzzy IF–THEN rules. FLCs can be classified into two major categories: the Mamdani type FLC that uses fuzzy numbers to make decisions and a Takagi– Segno (TS) type FLC that generates control actions by linear functions of the input variables. In the early years, most FLCs were designed by trial and error. Since the complexity of a FLC increases exponentially when it is be used to control complex systems. Hybridization of these two controller structures comes to one's mind immediately to exploit the beneficial sides of both categories. The two control structures are combined by a switch. In a fuzzy switching method between fuzzy controller and conventional PID controllers is used to achieve smooth control during switching. The motive to design a new hybrid fuzzy PID controller so that a further improved system response performance in both the transient and steady states can been achieved as compared to the system response obtained when either the classical PID or the fuzzy controller has been implemented.

Classical PID controller is the most popular control tool in many industrial applications because they can improve both the transient response and steady state error of the system at the same time. Moreover, it has simple architecture and conceivable physical intuition of its parameter. Traditionally, the parameters of a classical PID controller, i.e. KP, KI, and KD, are usually fixed during operation. Consequently, such a controller is inefficient for control a system while the system is disturbed by unknown facts, or the surrounding environment of the system is changed (Panichkun&Ngaechroenkul, 2000; Pratumsuwan et al, 2010). Fuzzy control is robust to the system with variation of system dynamics and the system of model free or the system which precise information is not required. It has been successfully used in the complex ill-defined process with better performance than that of a PID controller. Another important advance of fuzzy controller is a short rise time and a small overshoot (Aliyariet al, 2007; Panichkun&Ngaechroenkul, 2000). However, PID controller is better able to control and minimize the steady state error of the system. To enhance the controller performance, hybridization of these two controller structures comes to one mind immediately to exploit the beneficial sides of both categories, know as a hybrid of fuzzy and PID controller (Panichkun&Ngaechroenkul, 2000;Pratumsuwanetal, 2010).

Nevertheless, a hybrid of fuzzy and PID does not perform well when applied to the SEHS, because when the SEHS parameters changes will require new adjustment of the PID gains.

During the design of fuzzy based hybrid controller, the designer meets two key design challenges namely, optimization of existing fuzzy rule base and identification, estimation of new membership function or optimization of existing membership function. These issues play a vital role in controller design in real time. In real time controller hardware design there is memory and computational power constraints, so a designer needs to optimize these two design aspects.

Recent research into fuzzy control has applied classical techniques to stability analysis and design. The operation of a fuzzy controller behaves similar to a classical PD or PI controller. For a classical PD controller, the position and derivative gains remain constant for all values of input. However, for a fuzzy controller, the gains depend on the range where the control variables exist at any instant. The piecewise linearity of the fuzzy controller provides better system response than a classical controller. Also, since the operating point of the fuzzy controller is not fixed, it provides improved robustness to changes in the system parameters as compared to a classical controller.

Logically, it should be possible to divide the action of the PID controller into two separate control actions: PD controller for fastest response and PI controller for the elimination of the steady-state error. Obviously, the plant must be capable of being compensated by a PI controller. Figure 4.1 is the implementation of the proposed hybrid fuzzy PID control scheme. Similar to separate control rule tables for" coarse" and "fine" control, a PD controller provides the "coarse" control and the PI controller gives the "fine" control. The PI portion activates only when the PD portion reduces the error and change in error to where both are in the ZO fuzzy subset range. Therefore, at any instant, calculation of the control action involves only four control rules where as a three control variable controller (i.e. a typical PID) requires eight. If the three control variables of the hybrid controller contain seven

subsets each, only a maximum of sixteen subsets would be checked to determine the applicable rules. The rule search first checks the two ZO subsets for the PD portion and then checks at most all fourteen of the PI portion subsets. For the hybrid fuzzy PID controller, the PD and PI portions are designed separately and logic controls when to switch between the two controllers. The logic switches to the PI portion when both change of error and error are in the ZO range. The PD portion must not be re-enabled until the error variable moves out of the ZO range, regardless of the change in error variable. The PI portion in the process of reaching steady-state obviously creates a change in error that might be out of the PD's ZO range and thus reactivate the PD portion.

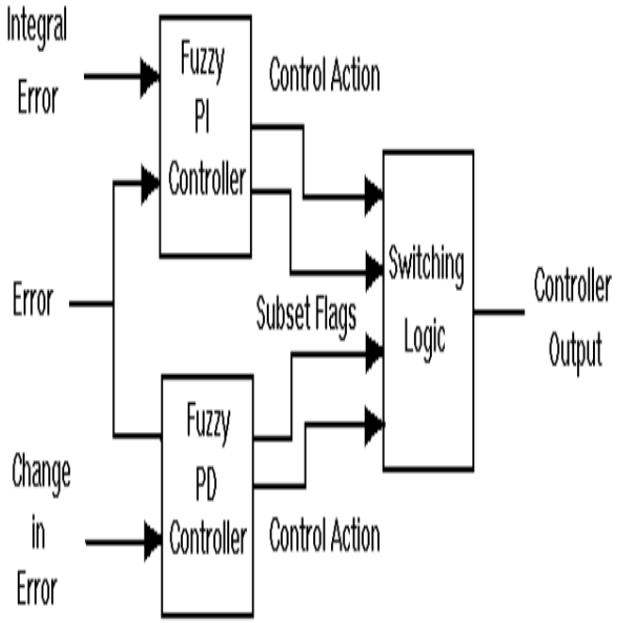

Figure 13 Hybrid PID Fuzzy Logic Controller

4.2.2 Hybrid Fuzzy-PID Controller

Although it is possible to design a fuzzy logic type of PID controller by a simple modification of the conventional ones, via inserting some meaningful fuzzy logic IF- THEN rules into the control system, these approaches in general complicate the overall design and do not come up with new fuzzy PID controllers that capture the essential characteristics and nature of the conventional PID controllers. Besides, they generally do not have analytic formulas to use for control specification and stability analysis. The fuzzy PD, PI, and PI+D controllers to be introduced below are natural extensions of their conventional versions, which preserve the linear structures of the PID controllers, with simple and conventional analytical formulas as the final results of the design. Thus, they can directly replace the conventional PID controllers in any operating control systems (plants, processes).

The main difference is that these fuzzy PID controllers are designed by employing fuzzy logic control principles and techniques, to obtain new controllers that possess analytical formulas very similar to the conventional digital PID controllers.

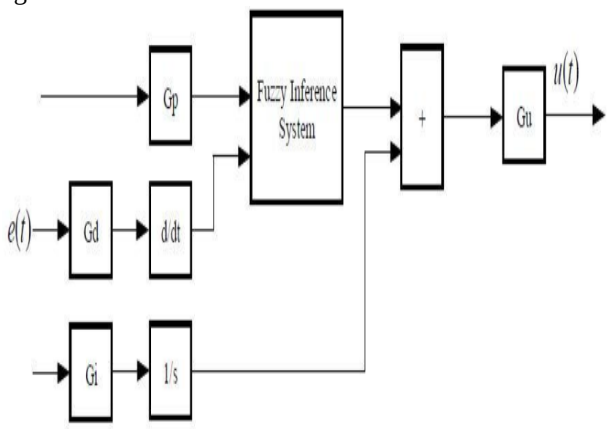

Figure 14: Hybrid Fuzzy PID Controller

VII MATLAB/SIMULATION RESULTS

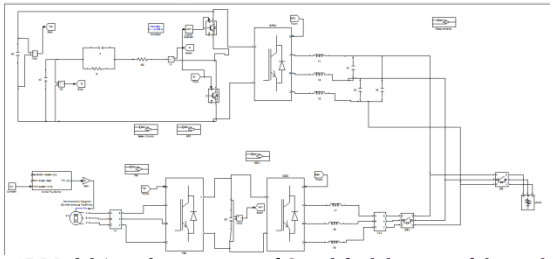

Fig 15 Matlab/simulation circuit of Simplified diagram of the studied microgrid.

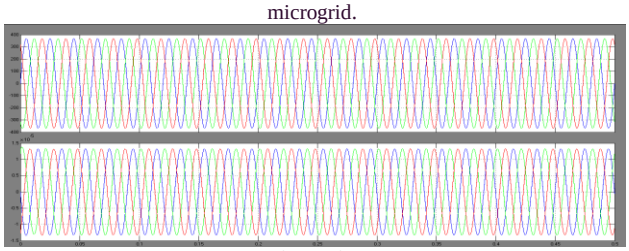

Fig 16 simulation wave form of grid voltage and current

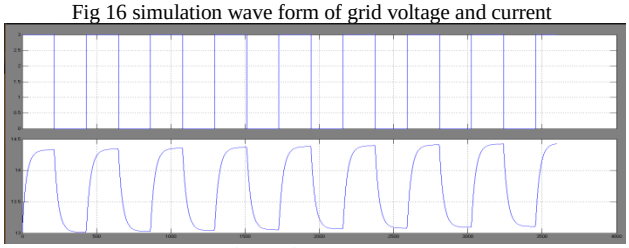

Fig 17 simulation wave form of during the tests with a 30-Ah 12-V lead–acid battery Current and Voltage

International Journal of Research
Available at https://edupediapublications.org/journals
e-ISSN: 2348-6848
p-ISSN: 2348-795X
Volume 05 Issue 12
April 2018

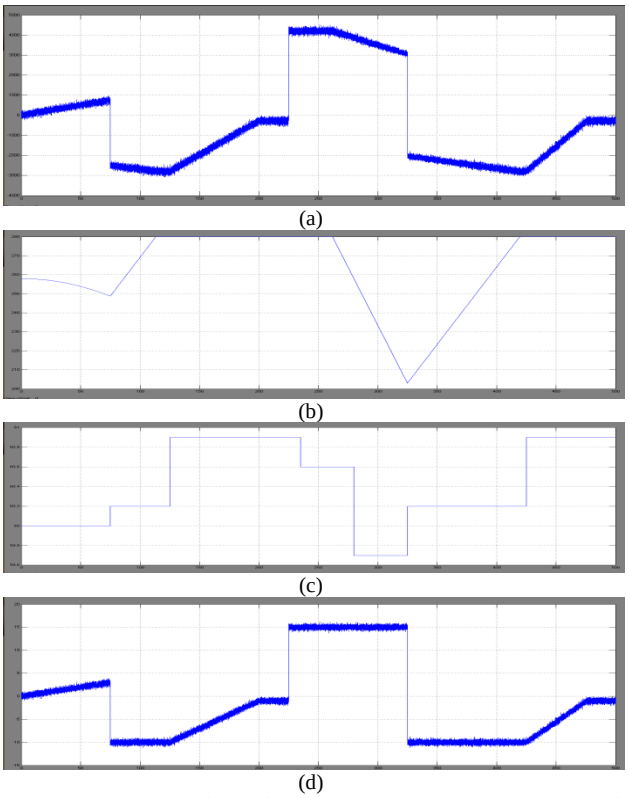

(a) (b) (c) (d)

Fig 18simulation wave form of Operation with a constant wind speed of 9.2 m/s: (a) Power at the GFC terminals, (b) battery bank voltage, (c) microgrid frequency, and (d) battery current

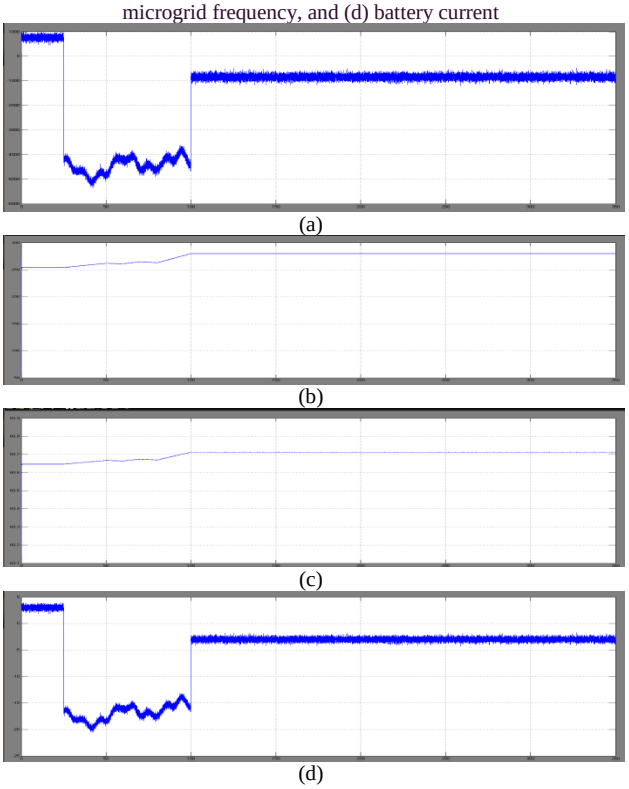

(a) (b) (c) (d)

Fig 19 simulation wave form of peration with variable wind speed: (a) Power at the GFC terminals, (b) battery bank voltage, (c) microgrid frequency, and (d) battery current.

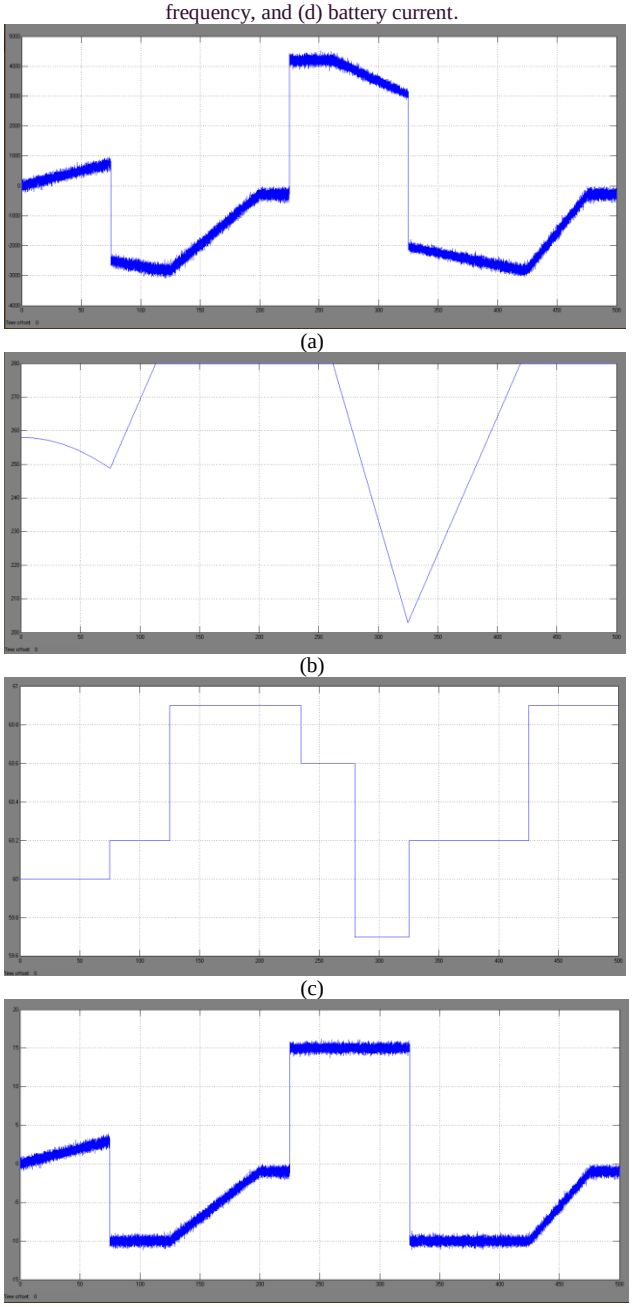

(a) (b) (c) (d)

Fig 20 simulation wave form of operation with variable wind speed with HYBRID fuzzy controller : (a) Power at the GFC terminals, (b) battery bank voltage, (c) micro grid frequency, and (d) battery current

VIII CONCLUSION

This paper proposed controller is a strategy to hybrid fuzzy logic control the generated power in order to keep the charging voltage battery banks under control in stand-

alone micro grid with distributed renewable energy sources. This strategy does not need wired communication between the distributed renewable sources nor dump loads to dissipate the surplus of generated power in the microgrid. These technical advantages make the proposed strategy a promising tool to increase the viability and reliability of the renewable power generation system installed in isolated and remote communities. Although a wind turbine has been used to demonstrate the validity of the proposed strategy, it is also valid regardless of the power source existing in the isolated microgrid. The proposed strategy calculates the amount
of power that must be generated at each time by each source in order to keep the balance of energy into the micro grid. In other words, the sum of the generated, consumed, and stored energy must always be zero all the time

REFERENCES

[1].José G. de Matos, Member, IEEE, Felipe S. F. e Silva, Student Member, IEEE, and Luiz A. de S. Ribeiro, Member, IEEE" Power Control in AC Isolated Micro grids With Renewable Energy Sources and Energy Storage Systems" IEEE Transactions On Industrial Electronics, Vol. 62, No. 6, June 2015.

[2] L. A. de S. Ribeiro, O. R. Saavedra, S. L. de Lima, and J. G. de Matos, "Isolated micro-grid with renewable hybrid generation: The case of Lençóis island," IEEE Trans. Sustain. Energy, vol. 2, no. 1, pp. 1–11, Jan. 2011.

[3] L. A. de S. Ribeiro, O. R. Saavedra, S. L. de Lima, and J. G. de Matos, "Making isolated renewable energy systems more reliable," Renew. Energy, vol. 45, pp. 221–231, Sep. 2012.

[4] J. G. de Matos, L. A. de S. Ribeiro, and E. C. Gomes, "Power control in ac autonomous and isolated micro grids with renewable energy sources and energy storage systems," in Proc. IEEE IECON, 2013, pp. 1827–1832.

[5] N. Mendis, K. M. Muttaqi, S. Pereira, and M. N. Uddin, "A novel control strategy for stand-alone operation of a wind dominated RAPS system," in Proc. IEEE IAS Annu. Meeting, 2011, pp. 1–8.

[6] J. Chen, J. Cheng, C. Gong, and X. Deng, "Energy management and power control for a stand-alone wind energy conversion system," in Proc. IEEE IECON, 2012, pp. 989–994.

[7] M. J. Erickson and R. H. Lasseter, "Integration of battery storage element in a CERTS microgrid," in Proc. IEEE ECCE, 2010, pp. 2570–2577.

[8] J. Rocabert, J. A. Luna, F. Blaabjerg, and P. Rodrígues, "Control of power converters in ac microgrids," IEEE Trans. Power Electron., vol. 27, no. 11, pp. 4734–4749, Nov. 2012.

[9] C. Jin, P. Wang, J. Xiao, Y. Tang, and F. H. Choo, "Implementation of hierarchical control in dc microgrids," IEEE Trans. Ind. Electron., vol. 61, no. 8, pp. 4032–4042, Feb. 2014.

[10] X. Lu, K. Sun, J. M. Guerrero, J. C. Vasquez, and L. Huang, "State-ofcharge balance using adaptive droop control for distributed energy storage systems in dc microgrid applications," IEEE Trans. Ind. Electron., vol. 61, no. 6, pp. 2804–2815, Jun. 2014.

[11] M. A. Abusara, J. M. Guerrero, and S. M. Sharkh, "Line-interactive UPS for microgrids," IEEE Trans. Ind. Electron., vol. 61, no. 3, pp. 1292–1300, Mar. 2014.

[12] J. M. Guerrero, P. X. Loh, T.-L. Lee, and M. Chandorkar, "Advanced control architectures for intelligent micro grids–Part II: Power quality, energy storage, ac/dc microgrids," IEEE Trans. Ind. Electron., vol. 60, no. 4, pp. 1263–1270, Apr. 2013.

[13] Z. Chen, J. M. Guerrero, and F. Blaabjerg, "A review of the state of art of power electronics for wind turbines," IEEE Trans. Power Electron., vol. 24, no. 8, pp. 1859–1875, Aug. 2009.